

# How Network Topology Affects the Strength of Dangerous Power Grid Perturbations

Calvin Alvares and Soumitro Banerjee

Department of Physical Sciences, Indian Institute of Science Education and Research  
Kolkata, Mohanpur, 741 246, India

E-mail: [alvarescalvin16@gmail.com](mailto:alvarescalvin16@gmail.com)

September 2024

**Abstract.** Reasonably large perturbations may push a power grid from its stable synchronous state into an undesirable state. Identifying vulnerabilities in power grids by studying power grid stability against such perturbations can aid in preventing future blackouts. Probabilistic stability quantifiers such as *basin stability*, which measures the asymptotic stability of a system, and *survivability*, which measures the transient stability of a system, have been commonly used to quantify the stability of nodes in a power grid. However, these quantifiers do not provide information about the strength of perturbations that destabilize the system. To measure the strength of perturbations beyond which the stability of the system gets compromised, we employ two probabilistic distance-based stability measures — *basin stability bound*, which deals with a system’s asymptotic behaviour, and *survivability bound*, a newly defined stability measure that deals with a system’s transient behaviour. Using these stability quantifiers, we conduct a detailed study on the impact of network topology on the strength of dangerous power grid perturbations. We find that certain tree-like structures and node connectivity can strongly predict nodes with low asymptotic and transient stability; we highlight network structures that are particularly vulnerable.

*Keywords:* power grids, probabilistic methods, network dynamics, stability of dynamical systems, coupled oscillator networks

## 1. Introduction

Power grids are critical infrastructures that underpin the functioning of modern society. Failures in these systems have resulted in large-scale blackouts that have left millions of people without electricity [1, 2, 3]. In recent times, grid expansion, modernization, and decentralization have been promoting rapid change to existing power grid infrastructure [4, 5, 6]. Thus, as power grids are becoming increasingly more complex, it is important to ensure they are resilient to various perturbations in order to prevent future blackouts.

During normal operation, all parts of a power grid function at the same frequency [7]. This state is called the grid’s synchronous state. Perturbations such as a line being

switched off or the power demand of the grid not being met may result in large parts of the grid desynchronizing, causing a cascading failure [8, 9, 10]. As perturbations affecting power grids can be reasonably large, linear stability analysis by means of evaluating the eigenvalues of the Jacobian matrix at an equilibrium point or the master stability function [11] cannot be employed as a measure of grid stability against such perturbations.

To quantify the stability of dynamical systems such as power grids against reasonably large perturbations, several non-local stability measures have been proposed [12, 13, 14, 15, 16, 17, 18]. Among these, a popular stability measure, known as *basin stability* [12], relates to the fraction of phase space that forms the basin of attraction of the desirable attractor. In the context of power grids, the desirable attractor corresponds to the grid's stable synchronous state. Basin stability has been used extensively in the study of power grid stability [19, 20, 21, 22, 23, 24, 25, 26].

Basin stability deals with the asymptotic, or, long term behaviour of a system. In addition to the asymptotic behaviour, the transient behaviour, that is, the behaviour of a system before it reaches its steady state, is particularly relevant when dealing with power grids. Power grids operate within certain frequency bounds, and control mechanisms are triggered when a perturbation causes the grid to operate out of the set frequency bound. Such perturbations are undesirable for the system. A stability measure called *survivability* has been proposed to quantify the transient stability of dynamical systems [13]. The set of states that do not leave a given desirable region of the phase space within a given time is called the *basin of survival*, and survivability is the fraction of states that are part of the system's basin of survival. Thus, survivability measures a system's capacity to resist perturbations from amplifying past the system's desirable region. Survivability, like basin stability, has been used to study power grid stability [13, 22, 27].

Basin stability and survivability are both volume-based measures of stability as they are related to the volume of the basin of attraction and the volume of the basin of survival, respectively. For power grids, the basin of attraction of the synchronous state can be very distorted [28]. It is possible that a stronger perturbation is safe for the system, but a weaker one is not. Hence, it is crucial to understand the magnitude of perturbations that are dangerous for the system. The volume-based stability measures fail to capture this. However, *basin stability bound* [29], a distance-based stability measure that provides a safe bound to the strength of perturbations based on the system's asymptotic behavior, captures this aspect. Analogous to basin stability bound, we propose a distance-based stability quantifier called *survivability bound* that provides a safe bound to the strength of perturbations based on the system's transient behaviour.

Using these two distance-based stability measures, we conduct a detailed study on the effect of network topology on power grid stability. Nodes with a low basin stability bound indicate that a low perturbation strength is required to cause permanent grid synchrony loss. On the other hand, nodes with a low survivability bound indicate that a low perturbation strength is required to cause undesirable transients in the system,

which do not necessarily lead to loss of grid synchrony. In this study, we outline the local network topology that results in low single-node stability.

This paper is organized as follows. The power grid model, methods of stability quantification, and a classification scheme of network nodes are presented in section 2. Section 3 describes the results, and section 4 concludes the work.

## 2. Methods

### 2.1. Power grid model

We use a complex network representation to model power grids with generators and consumers as nodes and transmission lines as edges. Generators and consumers are modelled as synchronous machines that follow the swing equation [7]. The equations that describe the dynamics of the grid are [30]

$$\dot{\theta}_i = \omega_i, \quad (1a)$$

$$I_i \dot{\omega}_i = -\gamma_i \omega_i + \bar{P}_i - \sum_{j=1}^N T_{ij} \sin(\theta_i - \theta_j), \quad (1b)$$

where  $\theta_i$  and  $\omega_i$  are the phase angle and the angular velocity of the synchronous machine at the  $i^{\text{th}}$  node of the power grid network in a frame rotating at the grid frequency.  $I_i$  is the inertia at the  $i^{\text{th}}$  node,  $\gamma_i$  is the damping at the  $i^{\text{th}}$  node, and  $\bar{P}_i$  is proportional to the net power generated or consumed at the  $i^{\text{th}}$  node.  $T_{ij}$  is the transmission capacity between node  $i$  and node  $j$ . If node  $i$  and node  $j$  are not connected, then  $T_{ij} = 0$ .

If all nodes have equal inertia ( $I_i = I$ ) and damping ( $\gamma_i = \gamma$ ), then the equations can be simplified as

$$\dot{\theta}_i = \omega_i, \quad (2a)$$

$$\dot{\omega}_i = -\alpha \omega_i + P_i - \sum_{j=1}^N K_{ij} \sin(\theta_i - \theta_j), \quad (2b)$$

where  $\alpha = \gamma/I$ ,  $P_i = \bar{P}_i/I$ ,  $K_{ij} = T_{ij}/I$ .

In this paper, we use the simplified differential equations described by equations (2a) and (2b) to model power grids. Each node in the network has two corresponding dynamical variables — a phase angle and a frequency. The fixed point of these equations corresponds to the stable synchronous state of the grid. In this state, the  $i^{\text{th}}$  node has a phase  $\theta_i^s$  and frequency 0 in the rotating frame of reference.

### 2.2. Basin stability bound

We first describe the basin stability bound introduced in [12, 19].

Consider an  $N$  dimensional dynamical system with a phase space  $X$ . The set  $\mathcal{A}$  is the system's desirable attractor. This attractor has a basin of attraction  $\mathcal{B}$ . Basin stability for the attractor  $\mathcal{A}$  is defined in a finite region of the phase space.

The basin stability of the attractor  $\mathcal{A}$ , defined in this finite region  $X^P$  is the fraction of states in the region  $X^P$  contained in the attractor's basin of attraction  $\mathcal{B}$ . The basin stability, assuming a uniform distribution of perturbations, is defined as

$$\beta(X^P) = \frac{\text{Vol}(\mathcal{B} \cap X^P)}{\text{Vol}(X^P)} \quad (3)$$

Thus, basin stability measures the probability that a perturbation in the region  $X^P$  causes the system to return to its desirable attracting state.

We consider a finite subset of the phase space  $X^0 \subseteq X$ , representing the extent to which perturbations can push the system. Basin stability bound is defined in this region  $X^0$ .

Let  $X^D(d)$  be the set of states within a distance  $d$  from the attractor  $\mathcal{A}$  that lie in the set  $X^0$ , i.e.,

$$X^D(d) = \{x \in X^0 \mid \text{dist}(x, \mathcal{A}) < d\} \quad (4)$$

where  $\text{dist}(x, \mathcal{A})$  is the distance of the state  $x$  to the attractor  $\mathcal{A}$ . In the case of the power grid model used in this paper, the attractor  $\mathcal{A}$  is a point attractor. The distance function  $\text{dist}(x, \mathcal{A})$  used in this paper is defined in section 2.4.

$D$  is the set of distances at which the corresponding basin stability is less than a basin stability tolerance  $t_\beta$ . Thus,

$$D_\beta = \{d \in (0, d_{\max}] \mid \beta(X^D(d)) < t_\beta\} \quad (5)$$

where  $t_\beta \in (0, 1]$  is a predefined basin stability tolerance, and  $d_{\max}$  is the maximum distance we would like to consider.

The basin stability bound of the attractor  $\mathcal{A}$  is defined as [29]

$$\bar{\beta} = \begin{cases} \inf(D_\beta) & \text{if } D_\beta \neq \emptyset \\ d_{\max} & \text{otherwise} \end{cases} \quad (6)$$

Thus, the basin stability bound is the minimum distance at which the corresponding basin stability is less than the tolerance  $t_\beta$ .

Single-node basin stability bound is defined as the basin stability bound with perturbations applied at a single network node starting from the initial attracting state. For a power grid, we consider a perturbation to  $\theta_i$  as a single-node perturbation at node  $i$ . If single-node perturbations occur in the region  $X^{sn}$ , such that  $\theta_i \in X^{sn}$  is a single-node perturbation at the  $i^{\text{th}}$  node; then the single-node basin stability bound of node  $i$  of the grid network is the basin stability bound defined in the region.

$$X_i^0 = \{(\theta, \omega) \in X \mid (\theta_i \in X^{sn} \wedge \omega_i = 0 \wedge (\forall j \neq i : \theta_j = \theta_j^s \wedge \omega_j = 0))\} \quad (7)$$

where  $\theta = (\theta_1, \theta_2, \dots, \theta_N)$  and  $\omega = (\omega_1, \omega_2, \dots, \omega_N)$

Basin stability is estimated using a Monte Carlo simulation. In the region  $X^P$ , a number of initial conditions,  $n$ , are sampled from a uniform distribution. If the number of initial conditions that converge to the attractor  $\mathcal{A}$  is  $n_\beta$ , then the estimated basin stability of the attractor is

$$\hat{\beta}(X^P) = \frac{n_\beta}{n} \quad (8)$$

To compute the basin stability bound, the basin stability  $\hat{\beta}(X^D(d))$  is computed from  $d = d_{\max}$  to  $d = d_0$ , using  $n$  samples for every basin stability estimation.  $d_0$  is the largest distance such that  $\hat{\beta}(X^D(d_0)) = 1$ . For  $\hat{\beta}(X^D(d)) < t_\beta$ , the values of  $d$  are noted and added to a set  $D_\beta$ . The basin stability bound is computed using equation 6. Refer to the paper by Alvares et al. [29] for a detailed computation procedure and the error associated in basin stability bound's estimation.

### 2.3. Survivability bound

Suppose the system has a desirable region  $X^+ \subseteq X$  of the phase space. A perturbation is considered safe if the state does not leave the desirable region in a finite time  $t$ . Let  $X_t^S$  be the set of points in  $X^P$  that do not leave the desirable region  $X^+$  in the time  $t$ . Assuming a uniform distribution of perturbations in the region  $X^P$ , survivability is defined as [13, 22]

$$\sigma(X^P) = \frac{\text{Vol}(X_t^S)}{\text{Vol}(X^P)} \quad (9)$$

Survivability, thus, represents the probability that a perturbation in the region  $X^P$  remains in the desirable region.

Consider  $D_\sigma$  the set of distances at which the corresponding survivability is less than a survivability tolerance  $t_\sigma$ .

$$D_\sigma = \{d \in (0, d_{\max}] \mid \sigma(X^D(d)) < t_\sigma\} \quad (10)$$

where  $t_\sigma \in (0, 1]$  is a predefined survivability tolerance,  $d_{\max}$  is the maximum distance we would like to consider, and  $X^D(d)$  is given by equation (4).

We define the survivability bound of the attractor  $\mathcal{A}$  as

$$\bar{\sigma} = \begin{cases} \inf(D_\sigma) & \text{if } D_\sigma \neq \emptyset \\ d_{\max} & \text{otherwise} \end{cases} \quad (11)$$

Thus, the newly proposed stability quantifier — survivability bound is the minimum distance at which the corresponding survivability is less than the tolerance  $t_\sigma$ .

In the case of the power grids, the desirable region is defined to be

$$X^+ = \{(\theta, \omega) \in X \mid \forall i : -\pi < \theta_i < \pi \wedge -\omega^+ < \omega_i < \omega^+\} \quad (12)$$

where  $\theta = (\theta_1, \theta_2, \dots, \theta_N)$  and  $\omega = (\omega_1, \omega_2, \dots, \omega_N)$  and  $\omega^+$  is a set bound to the frequency fluctuation.

If single-node perturbations occur in the region  $\theta_i \in X^{sn}$ , then the single-node survivability bound of node  $i$  is the survivability bound defined in the phase space region given by equation (7).

Survivability is estimated using a Monte Carlo simulation. In the region  $X^P$ , a number of initial conditions,  $n$ , are uniformly sampled. If the number of initial conditions that converge to the attractor  $\mathcal{A}$  is  $n_\sigma$ , then the estimated survivability is

$$\hat{\sigma} = \frac{n_\sigma}{n} \quad (13)$$

The survivability bound is computed using the same procedure used to compute the basin stability bound.

#### 2.4. Quantifying the strength of power grid perturbations

Basin stability bound and survivability bound rely on a notion of distance between a perturbed state and the attractor. This distance is indicative of the strength of perturbation. Distance in the phase space of a dynamical system can be quantified in various ways, ranging from standard Euclidean distance to the energy difference between the two states [29, 31]. For the distance of a perturbation from the synchronous state to have a physical meaning, we quantify it by defining an energy function that is related to the energy change of the system due to the perturbation.

Note that we have used a simplified power grid model given by equations (2a) and (2b) with the inertia at all nodes being the same and quantities such as torque and energy that we refer to are normalized by inertia.

Consider a perturbation in the phase angle  $\theta_i$  at the node  $i$  from the stable state value of  $\theta_i = \theta_i^s$  to  $\theta_i = \theta_i^p$ . It can be that either  $\theta_i^s < \theta_i^p$  or  $\theta_i^s > \theta_i^p$ . We assume that no energy is transferred back from the system in the process of perturbing  $\theta_i$ . The work  $W(\theta_i^s, \theta_i^p)$  done in moving from  $\theta_i^s$  to  $\theta_i^p$  is

$$W(\theta_i^s, \theta_i^p) = \int_{\theta_i^s}^{\theta_i^p} \tau(\theta_i) d\theta_i \quad (14)$$

where, as per the above assumption,

$$\tau(\theta_i) = \begin{cases} -\min\{0, \frac{d^2\theta_i}{dt^2}\} & \text{if } \theta_i^p > \theta_i > \theta_i^s \\ -\max\{0, \frac{d^2\theta_i}{dt^2}\} & \text{if } \theta_i^p < \theta_i < \theta_i^s \end{cases} \quad (15)$$

Additionally, we also assume that the perturbation is made at the synchronous grid frequency, which makes  $w_i = 0$ . The torque required for this is

$$\tau(\theta_i) = \begin{cases} -\min\{0, (P_i - \sum_{j=1}^N K_{ij} \sin(\theta_i - \theta_j))\} & \text{if } \theta_i^p > \theta_i > \theta_i^s \\ -\max\{0, (P_i - \sum_{j=1}^N K_{ij} \sin(\theta_i - \theta_j))\} & \text{if } \theta_i^p < \theta_i < \theta_i^s \end{cases} \quad (16)$$

The perturbation from  $\theta_i^s$  to  $\theta_i^p$  can happen through two different paths. For  $\theta_i^p > \theta_i^s$ , the two possible paths are  $\theta_i^s \rightarrow \theta_i^p$  and  $\theta_i^s \rightarrow -2\pi + \theta_i^p$ . For  $\theta_i^p < \theta_i^s$ , the two possible paths are  $\theta_i^s \rightarrow \theta_i^p$  or  $\theta_i^s \rightarrow 2\pi + \theta_i^p$ . We define energy  $E(\theta_i^p)$  as the energy of the perturbation from  $\theta_i^s$  to  $\theta_i^p$  along the path corresponding to the least energy change. Thus,

$$E(\theta_i^p) = \begin{cases} \min\{W(\theta_i^s, \theta_i^p), W(\theta_i^s, -2\pi + \theta_i^p)\} & \text{if } \theta_i^p > \theta_i^s \\ \min\{W(\theta_i^s, \theta_i^p), W(\theta_i^s, 2\pi + \theta_i^p)\} & \text{if } \theta_i^p < \theta_i^s \end{cases} \quad (17)$$

The distance between the perturbed state and the attractor is taken as the energy change of the system corresponding to a perturbation in the phase  $\theta_i^p$  at node  $i$  from the initial stable state. Thus,

$$\text{dist}(x_i^p, \mathcal{A}) = E(\theta_i^p) \quad (18)$$

where  $x_i^p = (\theta_1^s, \theta_2^s, \dots, \theta_i^p, \dots, \theta_N^s, 0, 0, \dots, 0, \dots, 0)$

### 2.5. Network motifs

J. Nitzbon et al. [22] have identified some important network motifs relevant to studying power grid stability. These network motifs are described below.

Consider a graph  $G = (V, E)$  with vertices  $V$  and edges  $E$ .  $G = (V, E)$  is a tree if it is connected and has no cycles.  $T' = (V', E')$  is a tree-shaped part of  $G$  if it is an induced subgraph of  $G$ , is a tree and is maximal with the property that there is exactly one node  $r \in V'$  that has at least one neighbour in  $G - T'$ . The node  $r$  of  $T'$  is called a root node ( $R$ ). The union of all tree-shaped parts of the graph  $G$  is called the forest  $T$  of the graph  $G$ . For a tree-shaped part, the depth of node  $x$  is the length of the shortest path from node  $x$  to the root node.

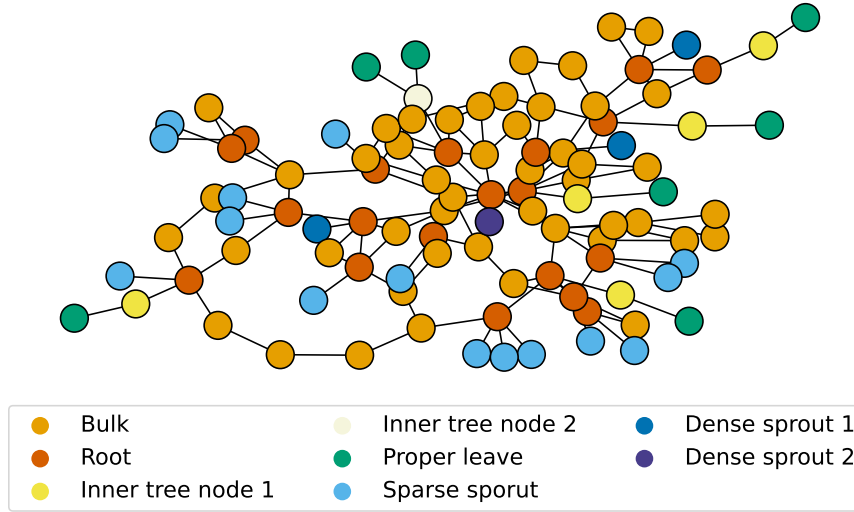


Figure 1: A network with nodes classified as bulk nodes, root nodes, inner tree nodes (class 1 and class 2), proper leaves, sparse sprouts, and dense sprouts (class 1 and class 2).

Nodes that do not belong to the forest part  $T$  are called bulk nodes ( $B$ ). Nodes that belong to the forest part and are not root nodes are called non-root nodes. Non-root nodes that have a degree greater than one are called inner tree nodes ( $I$ ). Non-root nodes that have a degree of one are called leaves. Leaves that have a depth of more than one are proper leaves ( $P$ ), and leaves that have a depth of one are called sprouts. Sprouts with an average neighbour degree of less than six are called sparse sprouts ( $S_s$ ), and sprouts with an average neighbour degree of more than five are called dense sprouts ( $S_d$ ). Fig. 1 shows a network with nodes classified as described above.

We further divide the inner leaf nodes into two classes. Class 1 inner tree nodes are inner tree nodes with a degree of two, and class 2 inner leaf nodes are inner tree nodes with a degree greater than two. We also divide dense sprouts into two classes. Class 1 dense sprouts are dense sprouts with a degree of six and seven, and class 2 dense sprouts have a degree greater than six.

### 3. Results

We use a random network generator model proposed by Schultz et al. [32] to generate realistic power grid networks to study the effect of network topology on power grid stability. The parameters chosen for this model are  $N_0 = 1$ ,  $p = 1/5$ ,  $q = 3/10$ ,  $s = 1/3$ ,  $t = 1/10$ . 50 such networks, each consisting of 100 nodes, were generated. In each network, half of the nodes were taken to be generators, and half of the nodes were taken to be consumers. Grid networks were modelled using equations (2a) and (2b), with the following parameters:  $K = 6$  for every transmission line,  $\alpha = 0.1$  for every node,  $P = 1$  for every generator, and  $P = -1$  for every consumer. One unit of time in the differential equations corresponds to 0.25 s. Using this ensemble of grid networks, we investigate the single-node basin stability bound and the single-node survivability bound for every node of all the networks.

Deviations in the grid frequency of power grids are generally kept within  $\pm 1$  Hz. A deviation of  $\pm 1$  Hz in the frequency corresponds to a  $\omega \approx \pm 1.57$  in the units we have used. We choose two values for the desirable region's frequency bound  $\omega^+$ . We choose  $\omega^+ = 1$  corresponding to an allowed frequency deviation of  $\pm 0.64$  Hz. Another value  $\omega^+ = 5$ , corresponding to an allowed frequency deviation of  $\pm 3.2$  Hz, is chosen to investigate how the survivability bound changes when large frequency deviations are allowed. The region  $X^{sn} = [-\pi, \pi]$  represents single-node perturbations in the phase angle. The single-node basin stability bound and single-node survivability bound of node  $i$  in a network are computed in the region  $X_i^0$  given by equation (7) for single-node perturbations in the region  $X^{sn}$ . Basin stability bound and survivability bound are computed using tolerances  $t_\beta = 0.95$  and  $t_\sigma = 0.95$ , respectively, and the maximum perturbation distance limit is set to  $d_{\max} = 50$ . For all basin stability and survivability computations,  $n = 200$  initial conditions were used, and every initial condition was evolved for time  $t = 100$ . Numerically, a perturbation is counted to be in the basin of attraction if  $|\omega_i| < 1 \forall i$  at  $t = 100$ .

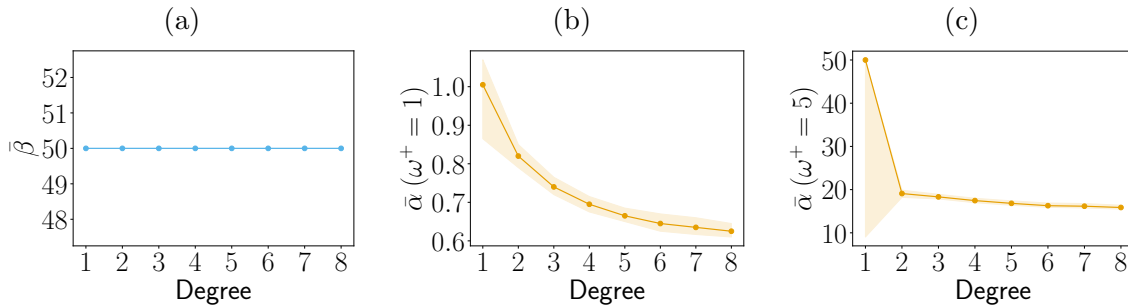


Figure 2: The dependence of single-node stability on degree. (a) Basin stability bound versus degree. (b) Survivability bound ( $w^+ = 1$ ) versus degree. (c) Survivability bound ( $w^+ = 5$ ) versus degree. The dots show the average value, and the shaded region indicates the 15.9% to the 84.1% percentile.



Fig. 2 shows the relationship between degree and single-node stability. Fig. 2a does not show a correlation between basin stability bound and a node's degree. Nodes with low basin stability bound are not captured by this plot as their values lie below the 15.9% percentile range; these nodes are better examined by looking at the basin stability bound values for different network motifs. Fig. 2b shows the dependence of survivability bound on degree — a strong negative correlation is seen. Fig. 2c also shows a negative correlation with survivability bound and degree. However, nodes with a degree of one show variable values of survivability bound. Nodes of degree one can be further bifurcated into proper leaves, sparse sprouts, class 1 dense sprouts and class 2 dense sprouts. These node classes are examined to identify vulnerable network structures better.

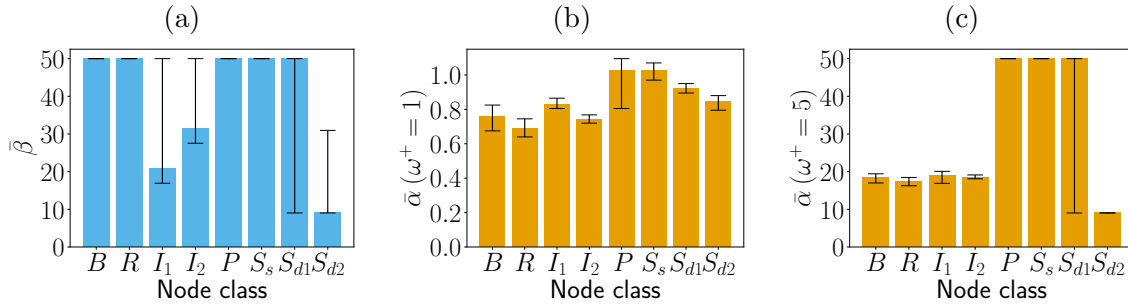


Figure 3: Bar graph showing the average single-node stability for bulk nodes ( $B$ ), root nodes ( $R$ ), class 1 inner tree nodes ( $I_1$ ), class 2 inner tree nodes ( $I_2$ ), proper leaves ( $P$ ), sparse sprouts ( $S_s$ ), class 1 dense sprouts ( $S_{d1}$ ) and class 2 dense sprouts ( $S_{d2}$ ). (a) Basin stability bound for each node class. (b) Survivability bound ( $w^+ = 1$ ) for each node class. (c) Survivability bound ( $w^+ = 5$ ) for each node class. The black line indicates the 15.9% to the 84.1% percentile.

Fig. 3 shows the average single-node stability values for the different classes of nodes. In Fig. 3a, we observe that class 1 and class 2 dense sprouts are the least stable nodes out of all the nodes with a degree of one. Additionally, Fig. 3a shows that class 1 and class 2 inner tree nodes have low stability bound values. In Fig. 3b, we observe that root nodes and bulk nodes have the lowest survivability bound values. These nodes are in the interior of networks and are thus generally well-connected and have a higher degree than other nodes. This agrees with the fact that survivability bound is negatively correlated with a node's degree (Fig. 2b). In Fig 3c, it is observed that dense sprouts have the lowest survivability bound values. Thus, as the allowed frequency deviations increase, dense sprouts move from having relatively high survivability values compared to other nodes to having the lowest survivability values.

## 4. Conclusion

In this work, we have employed asymptotic and transient stability quantifiers to measure the magnitude of dangerous single-node power grid perturbations. A perturbation stronger than a node's basin stability bound can be devastating for the grid, and can result in grid synchrony loss and cascading failure. On the other hand, a perturbation stronger than a node's survivability bound might be undesirable for the grid as it momentarily pushes node frequencies out of the desirable operation region without necessarily pushing the grid permanently out of synchrony.

We have studied the effect of network topology on single-node stability using these distance-based measures of stability, departing from commonly used volume-based stability quantifiers. Through the study of the single-node stability of an ensemble of synthetic power grids, we have identified vulnerable local network properties of power grids. We have found that inner leaf nodes and dense sprouts have the lowest values of basin stability bound. Hence, large perturbations to these nodes should be avoided at all costs. On the other hand, nodes with a high degree have low survivability bound values (when the tolerated frequency deviations in the grid are small ( $\pm 0.64$  Hz)). This means that perturbations to these nodes have the highest chance of resulting in undesirable transients in the grid but may rarely ever result in total loss of synchrony due to such nodes having high basin stability bound values. However, when the tolerated frequency deviations are larger ( $\pm 3.2$  Hz), dense sprouts have the lowest survivability values. Dense sprouts have the lowest basin stability bound and survivability bound values in this case.

We believe the methods used and the results obtained in this study can prove useful to future research on the stability of power grids and other complex networks.

## Acknowledgments

We thank Dr. Frank Hellmann from Potsdam Institute for Climate Impact Research, for his helpful suggestions. S B acknowledges the J C Bose National Fellowship provided by SERB, Government of India, Grant No. JBR/2020/000049.

## References

- [1] Central Electricity Regulatory Commission (CERC). Report on the grid disturbances on 30th July and 31st July 2012. Technical report, 2012.
- [2] Project Group Turkey. Report on blackout in Turkey on 31st March 2015. Technical report, European Network of Transmission System Operators for Electricity (ENTSO-E), 2015.
- [3] Union for the Coordination of Transmission of Electricity (UCTE). Final report of the investigation committee on the 28th September 2003 blackout in Italy. Technical report, European Network of Transmission System Operators for Electricity (ENTSO-E), 2003.
- [4] Guido Pepermans, Johan Driesen, Dries Haeseldonckx, Ronnie Belmans, and William D'haeseleer. Distributed generation: definition, benefits and issues. *Energy policy*, 33(6):787–798, 2005.

- [5] Maria Luisa Di Silvestre, Salvatore Favuzza, Eleonora Riva Sanseverino, and Gaetano Zizzo. How decarbonization, digitalization and decentralization are changing key power infrastructures. *Renewable and Sustainable Energy Reviews*, 93:483–498, 2018.
- [6] Xi Fang, Satyajayant Misra, Guoliang Xue, and Dejun Yang. Smart grid—the new and improved power grid: A survey. *IEEE communications surveys & tutorials*, 14(4):944–980, 2011.
- [7] Jan Machowski, Zbigniew Lubosny, Janusz W Bialek, and James R Bumby. *Power system dynamics: stability and control*. John Wiley & Sons, 2020.
- [8] Sergey V Buldyrev, Roni Parshani, Gerald Paul, H Eugene Stanley, and Shlomo Havlin. Catastrophic cascade of failures in interdependent networks. *Nature*, 464(7291):1025–1028, 2010.
- [9] Adilson E Motter and Ying-Cheng Lai. Cascade-based attacks on complex networks. *Physical Review E*, 66(6):065102, 2002.
- [10] Benjamin Schäfer, Dirk Witthaut, Marc Timme, and Vito Latora. Dynamically induced cascading failures in power grids. *Nature communications*, 9(1):1975, 2018.
- [11] Louis M Pecora and Thomas L Carroll. Master stability functions for synchronized coupled systems. *Physical review letters*, 80(10):2109, 1998.
- [12] Peter J Menck, Jobst Heitzig, Norbert Marwan, and Jürgen Kurths. How basin stability complements the linear-stability paradigm. *Nature physics*, 9(2):89–92, 2013.
- [13] Frank Hellmann, Paul Schultz, Carsten Grabow, Jobst Heitzig, and Jürgen Kurths. Survivability of deterministic dynamical systems. *Scientific reports*, 6(1):29654, 2016.
- [14] Chiranjit Mitra, Jürgen Kurths, and Reik V Donner. An integrative quantifier of multistability in complex systems based on ecological resilience. *Scientific reports*, 5(1):16196, 2015.
- [15] Chiranjit Mitra, Anshul Choudhary, Sudeshna Sinha, Jürgen Kurths, and Reik V Donner. Multiple-node basin stability in complex dynamical networks. *Physical Review E*, 95(3):032317, 2017.
- [16] Vladimir V Klinshov, Vladimir I Nekorkin, and Jürgen Kurths. Stability threshold approach for complex dynamical systems. *New Journal of Physics*, 18(1):013004, 2015.
- [17] Lukas Halekotte and Ulrike Feudel. Minimal fatal shocks in multistable complex networks. *Scientific reports*, 10(1):11783, 2020.
- [18] Vladimir V Klinshov, Sergey Kirillov, Jürgen Kurths, and Vladimir I Nekorkin. Interval stability for complex systems. *New Journal of Physics*, 20(4):043040, 2018.
- [19] Peter J Menck, Jobst Heitzig, Jürgen Kurths, and Hans Joachim Schellnhuber. How dead ends undermine power grid stability. *Nature communications*, 5(1):3969, 2014.
- [20] Peng Ji and Jürgen Kurths. Basin stability of the Kuramoto-like model in small networks. *The European Physical Journal Special Topics*, 223(12):2483–2491, 2014.
- [21] Paul Schultz, Jobst Heitzig, and Jürgen Kurths. Detours around basin stability in power networks. *New Journal of Physics*, 16(12):125001, 2014.
- [22] Jan Nitzbon, Paul Schultz, Jobst Heitzig, Jürgen Kurths, and Frank Hellmann. Deciphering the imprint of topology on nonlinear dynamical network stability. *New Journal of Physics*, 19(3):033029, 2017.
- [23] Heetae Kim, Sang Hoon Lee, and Petter Holme. Building blocks of the basin stability of power grids. *Physical Review E*, 93(6):062318, 2016.
- [24] Christian Nauck, Michael Lindner, Konstantin Schürholt, Haoming Zhang, Paul Schultz, Jürgen Kurths, Ingrid Isenhardt, and Frank Hellmann. Predicting basin stability of power grids using graph neural networks. *New Journal of Physics*, 24(4):043041, 2022.
- [25] Yannick Feld and Alexander K Hartmann. Large-deviations of the basin stability of power grids. *Chaos: An Interdisciplinary Journal of Nonlinear Science*, 29(11), 2019.
- [26] Benjamin Schäfer, Carsten Grabow, Sabine Auer, Jürgen Kurths, Dirk Witthaut, and Marc Timme. Taming instabilities in power grid networks by decentralized control. *The European Physical Journal Special Topics*, 225:569–582, 2016.
- [27] Anna Büttner, Jürgen Kurths, and Frank Hellmann. Ambient forcing: Sampling local perturbations in constrained phase spaces. *New Journal of Physics*, 24(5):053019, 2022.

- [28] Lukas Halekotte, Anna Vanselow, and Ulrike Feudel. Transient chaos enforces uncertainty in the British power grid. *Journal of Physics: Complexity*, 2(3):035015, 2021.
- [29] Calvin Alvares and Soumitro Banerjee. A probabilistic distance-based stability quantifier for complex dynamical systems. *Nonlinear Dynamics*, pages 1–12, 2024.
- [30] Giovanni Filatrella, Arne Hejde Nielsen, and Niels Falsig Pedersen. Analysis of a power grid using a Kuramoto-like model. *The European Physical Journal B*, 61:485–491, 2008.
- [31] Niklas LP Lundström. How to find simple nonlocal stability and resilience measures. *Nonlinear dynamics*, 93(2):887–908, 2018.
- [32] Paul Schultz, Jobst Heitzig, and Jürgen Kurths. A random growth model for power grids and other spatially embedded infrastructure networks. *The European Physical Journal Special Topics*, 223(12):2593–2610, 2014.